

### 5.1.3.2 Control of Ruthenium Particle Size by the Reverse Micelle Technique

#### 5.1.3.2.1 Catalysts with ~5 nm Ruthenium Particles

Several ruthenium catalysts were prepared in 2 g quantities by variations of the reverse micelle procedure using reverse micelle solutions similar to 4956-24-1.

Results of STEM examination of the first successful Catalyst 4956-19 (~1.7% Ru, by wt.) are shown in Figure 5-51 and Table 5-15. Over 90% of the ruthenium particles were in the 4-6 nm size range with a few large particles in the 11 to 13 nm size range. Two-thirds of the alumina particles that were examined were found to contain ruthenium.

Experiments were also done to determine the structure of some of the Ru particles in Catalyst 4956-19. The objective was to establish if Ru metal was maintained after exposing the sample to various handling procedures under  $N_2$ . The diffraction patterns are shown in Figures 5-52 and 5-53. The patterns, two of which are shown here, were generally of particles 4-12 nm in size. The pattern shown in Figure 5-52 was with a  $10\mu$  aperture, camera length of 2M at 20 MX. The zone axis is either [010], [101] or [121]. Figure 5-53 is a microdiffraction pattern of another 12.5 nm particle using the same instrumental conditions as above except a  $25\mu$  aperture was used. The zone axis is [121]. The objective apertures used in these experiments varies the angle of probe convergence. For the  $10\mu$  aperture the angle is  $3.6 \times 10^{-3}$  rad and for the  $25\mu$  aperture it is  $4.5 \times 10^{-3}$  rad. This was based on a procedure described by Warren [70]. Although only a few diffraction spots were observed, these spots indexed reasonably well for Ru metal. Figure 5-53 shows a partial hexagonal microdiffraction pattern which provides very strong evidence for the presence of Ru metal. Thus, it appears that the transfer technique works reasonably well in minimizing oxidation of Ru.

Figure 5-50

Guinier Plot for the Reverse Micelle Solution 4966-52

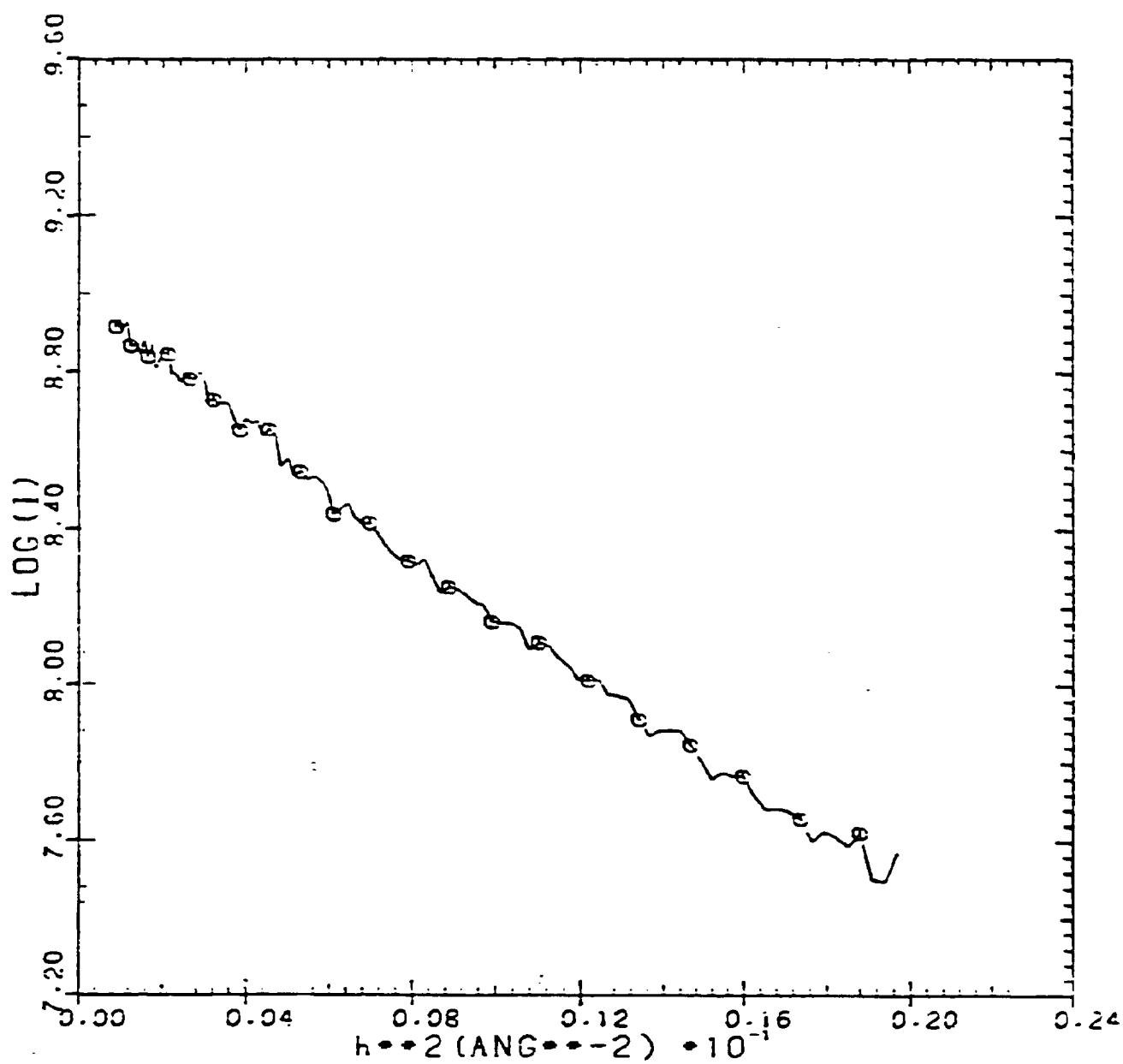


Figure 5-51

STEM Micrograph of Catalyst 4956-19

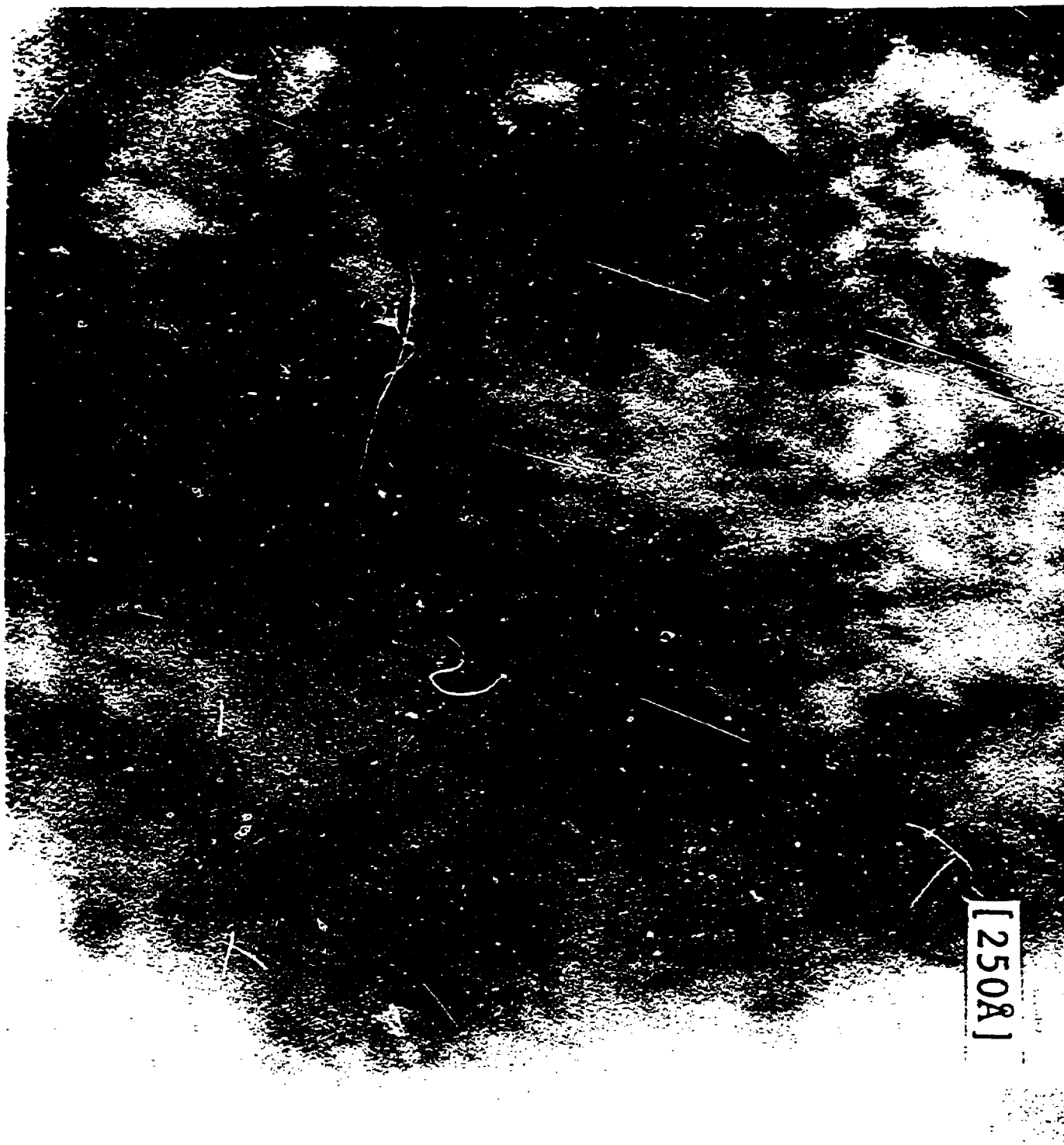


Table 5-15

Percent Ruthenium Analysis on  
Several Alumina Particles for Catalyst 4956-19

(Alumina Particles Containing Ruthenium)

Particle #	WEIGHT %			
	Al	RuL $\alpha$	Al	RuK $\alpha$
1	97.7	2.3		Y
2	99.1	0.9		Y
3	92.9	7.1		Y
4	98.4	1.6		Y
5	98.8	1.2		Y
6	82.7	17.3	85.5	14.5
7	80.0	20.0	75.1	24.9
8	80.6	19.4	76.9	23.1
9	90.4	9.6	92.8	7.2
10	98.0	2.0	97.8	2.2
11	98.4	1.6		Y
12	98.1	1.9		Y
13	98.9	1.1		Y
14	96.9	3.3	97.1	2.9
15	97.5	2.5	98.2	1.8
16	96.8	3.2		Y
17	97.3	2.7		Y
18	98.4	1.6		Y
19	98.1	1.9		Y
20	98.8	1.2		Y
21	99.0	1.0		N
22	100			N
23	99.4	0.6		N
24	99.2	0.8		N
25	98.7	1.3		N
26	99.0	1.0		N
27	99.2	0.8		N
28	99.3	0.7		N
29	98.9	1.1		N
30	98.9	1.1		N
31	99.0	1.0		N

Y - Designates small RuK $\alpha$  peak observed but not distinguished from background by the computer.

N - No RuK $\alpha$  line observed.

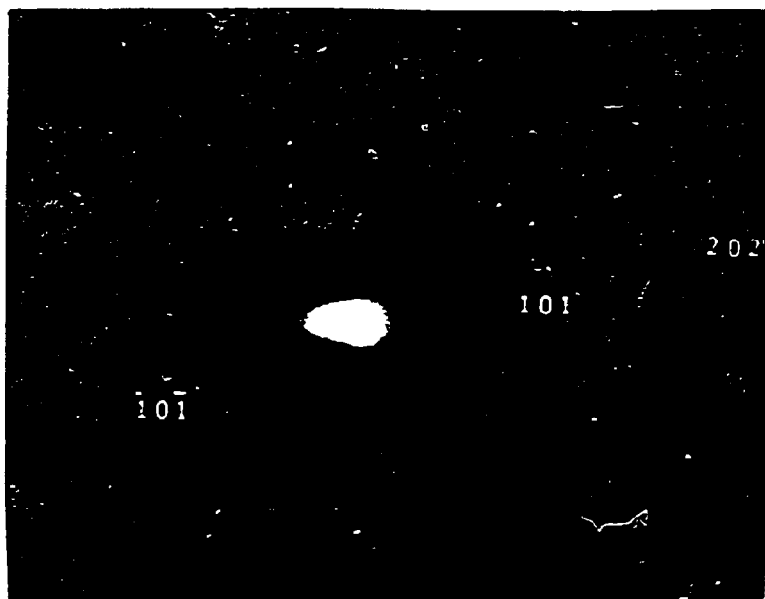


Figure 5-52      Microdiffraction of a 125Å  
Ru Crystallite at 20 MX



Figure 5-53      Microdiffraction of a 125Å  
Ru Crystallite at 20 MX

Similar ruthenium particle size distributions were obtained with reverse-micelle derived Catalysts 4956-21, 4956-69, 4956-70, 4956-71, all prepared in 2 g quantities at about 1 wt.% Ru level. Over 80-90% of the alumina particles examined in these catalysts had observable ruthenium particles.

Catalyst 4956-23 was the first attempt to make the catalyst in a 30 g quantity instead of 2 g. The ruthenium particle sizes varied from 4 to 100 nm (Figures 5-54 and 5-55).

Several other 30 g-batch catalysts were made unsuccessfully with similarly wide ruthenium particle size distributions.

Catalyst 4956-76 with 0.93 wt.% Ru was the first successful micelle-derived catalyst prepared in a 30 g quantity. STEM micrograph and size distribution results for Catalyst 4956-76 are shown in Figures 5-56 and 5-57. About 90% of the ruthenium particles were 4-6 nm in size. The remaining particles were 10-15 nm (5-7%) and 20-25 nm (3-5%). Also, 70-80% of the alumina particles that were examined contained observable ruthenium. The  $H_2:Ru$  and  $O:Ru$  ratios for this catalyst were 0.29 and 0.31, respectively.

After the early preparation of Catalyst 4956-76, several other large-batch catalysts were made with mostly 4-6 nm ruthenium particles. All of these catalysts, including 4956-76, were tested in the fixed-bed pilot plant.

Catalyst 4966-96-1 with 1.12% Ru, by wt., had observable ruthenium particles over 90% of the alumina particles. About 40-45% of the ruthenium particles were in the 3-4 nm size range, another 40-45% were in the 5-7 nm size range, while most of the rest of the ruthenium particles were 7-10 nm (Figures 5-58 and 5-59). The  $H_2:Ru$  and  $O:Ru$  ratios for this catalyst were 0.50 and 0.55, respectively.

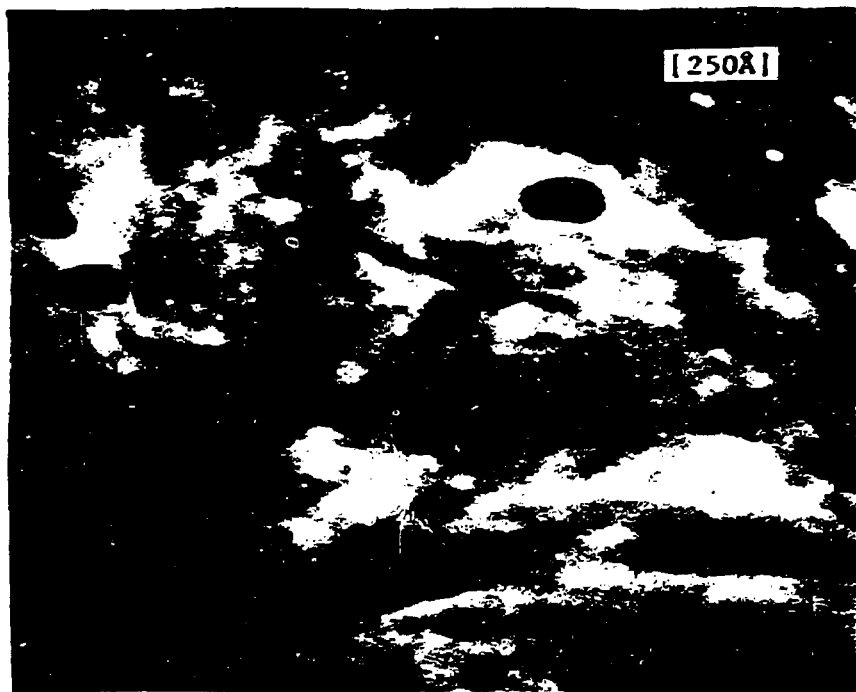
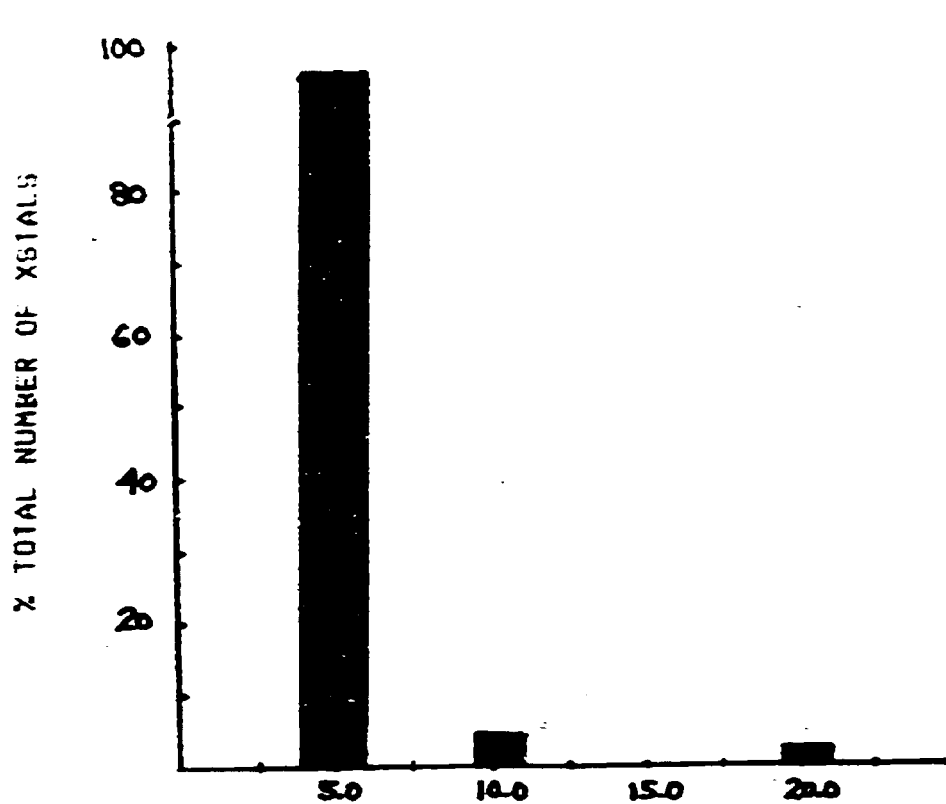


Figure 5-54. STEM Micrograph of Catalyst 4956-23



Figure 5-55. STEM Micrograph of Catalyst 4956-23

Figure 5-56



Ruthenium Particle Size Distribution for Catalyst 4956-76

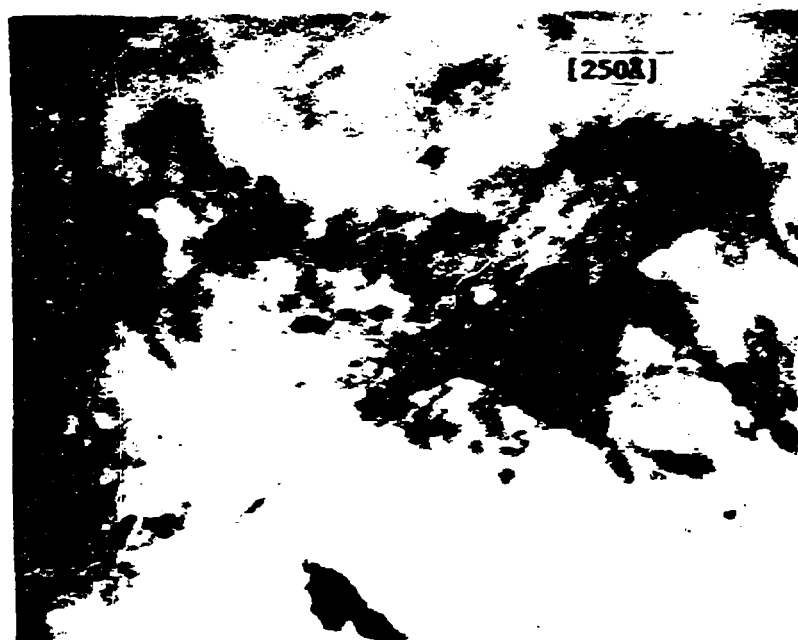


Figure 5-57

STEM Micrograph of Catalyst 4956-76



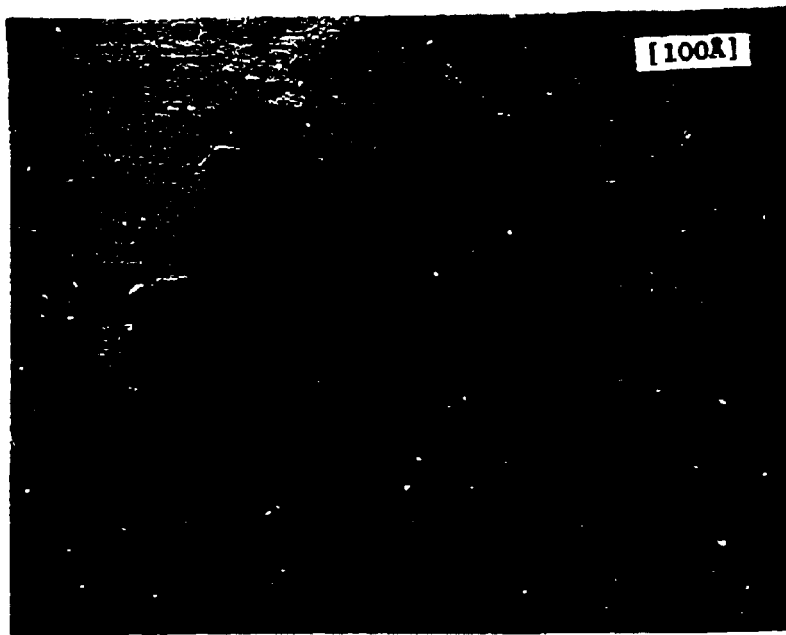


Figure 5-58. STEM Micrograph of Catalyst 4966-96-1



Figure 5-59. STEM Micrograph of Catalyst 4966-96-1

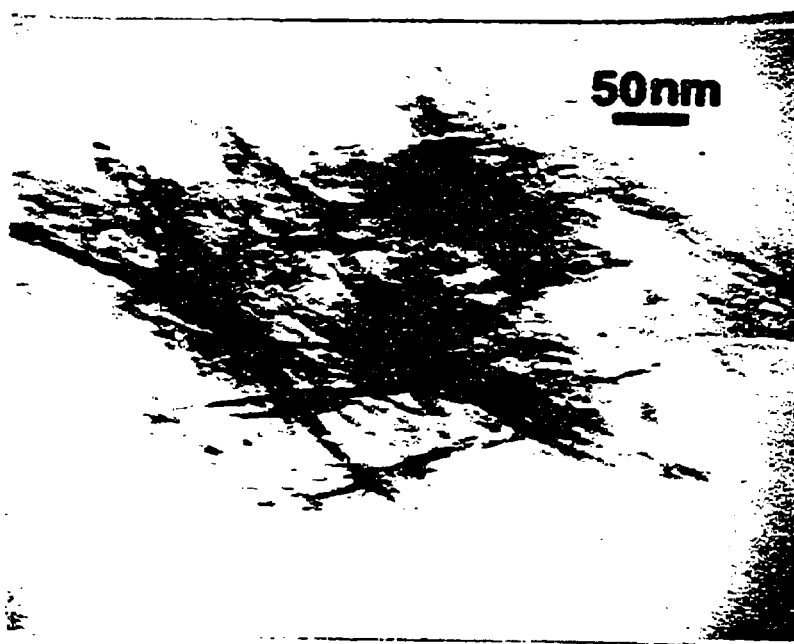
Over 90% of the alumina particles in Catalyst 4966-108 (1% Ru, by wt.) had observable ruthenium particles (Figure 5-60). Of these ruthenium particles 95% were 4-6 nm, while 5% were 10-15 nm.

Catalyst 4966-119 with 1.5% Ru (by wt.) had approximately 1/3 (by wt.) of the ruthenium in the form of 100 nm or larger particles, while the rest of the ruthenium was in the form of intermediate size particles. Of these intermediate size particles 80% were 4-6 nm and 20% were 8-10 nm in size.

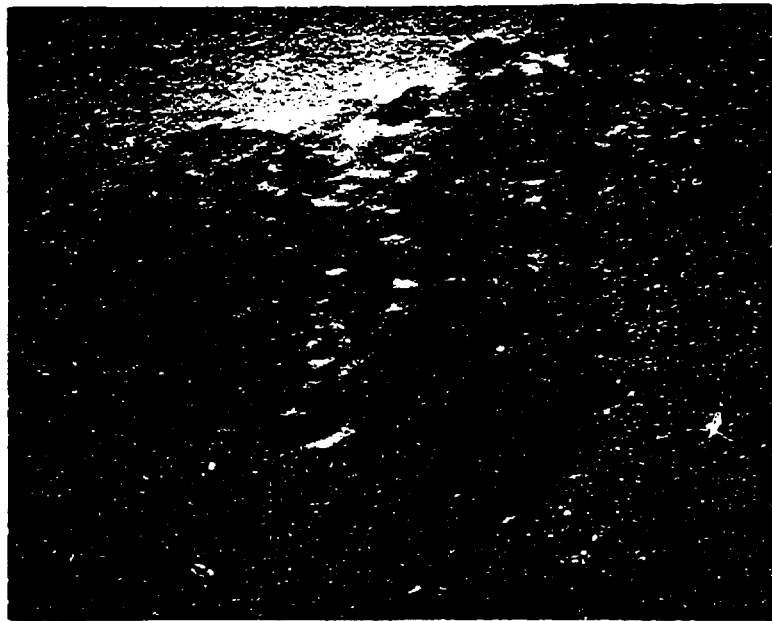
Catalyst 4966-198, which contained 3% Ru (by wt.) had observable ruthenium particles on over 90% of the alumina particles (Figures 5-61 and 5-62). Approximately 85% of the ruthenium particles were 4-6 nm, while the rest were 3-4 nm or 6-20 nm.

Figure 5-60

**STEM Micrograph of Ru/ $\gamma$ -Al<sub>2</sub>O<sub>3</sub> Catalyst  
with 4-6 nm Ruthenium Particles**



**FRESH**



**Figure 5-61. STEM Micrograph of Catalyst 4966-198**



**Figure 5-62. STEM Micrograph of Catalyst 4966-198**

#### 5.1.3.2.2 Catalysts with $\leq 2-4$ nm Ruthenium Particles on Alumina

Several ruthenium catalysts were prepared with the objective of making ruthenium particles smaller than 4-6 nm. For some of them, solutions with smaller reverse micelles, i.e., 4966-50, were used.

Catalyst 4966-102 with ~1% Ru (by wt.) and 0.5% Fe (by wt.) had 85% of the visible ruthenium-iron particles in the 2-4 nm size range, 10% in the 4-6 nm size range, and 5% in the 6-15 nm size range (Figures 5-63 and 5-64). The iron:ruthenium atomic ratio in the iron-ruthenium particles varied mostly between 0.3 and 1. Since the bulk iron:ruthenium atomic ratio was equal to 1, some of the iron must be on alumina in a highly dispersed form. EXAFS measurements indicated that the average particle size was 4 nm. The  $H_2$ :Ru+Fe atomic ratio was 0.26.

Catalyst 4956-101 with 0.86% Ru (by wt.) had some 2-4 nm particles (mostly 2-3 nm) according to the STEM examination (Figure 5-65). The  $H_2$ :Ru and O:Ru ratios were 0.54 and 0.59.

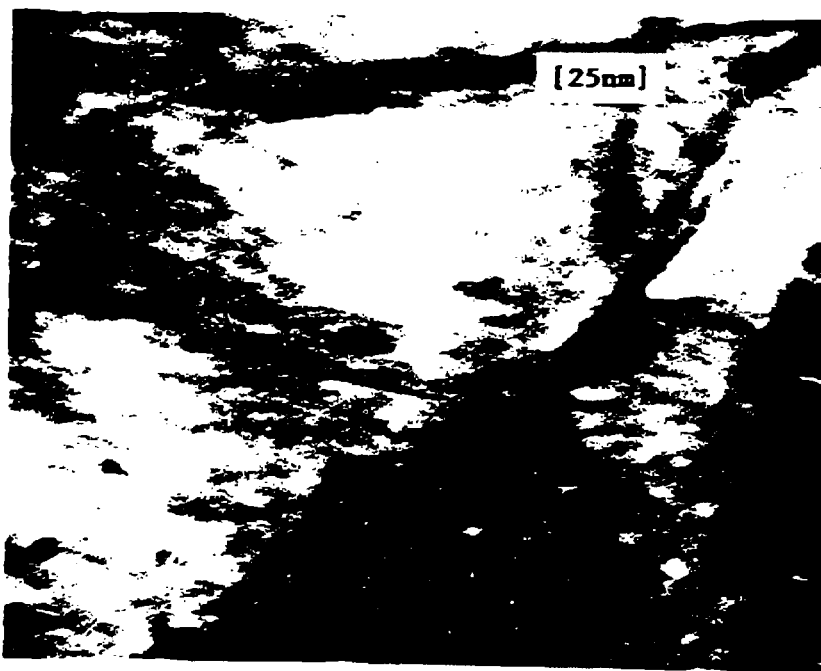


Figure 5-65. STEM Micrograph of Catalyst 4956-101



Figure 5-63. STEM Micrograph of Catalyst 4966-102

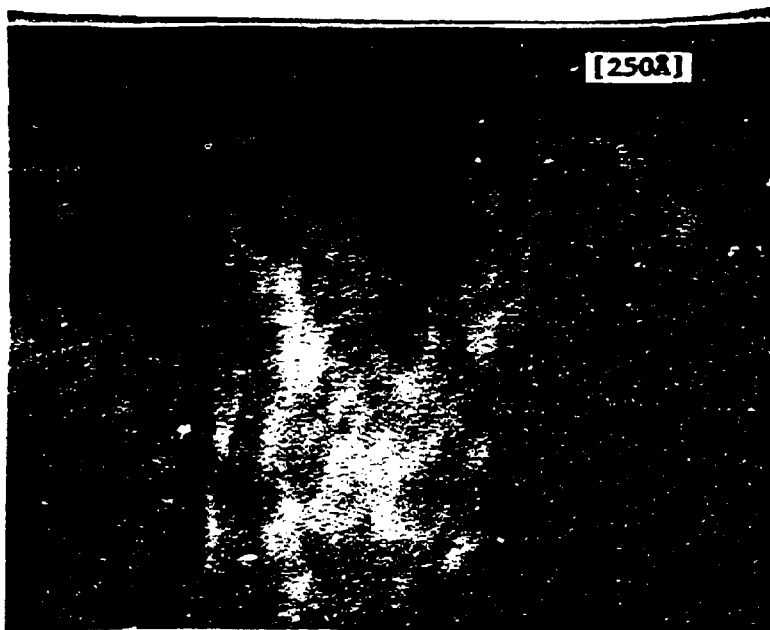


Figure 5-64. STEM Micrograph of Catalyst 4966-102

Catalyst 4966-76 with 0.84% Ru (by wt.) also had some 2-4 nm ruthenium particles in the STEM examination (Figure 5-66). According to EXAFS measurements, the average ruthenium particle size in Catalyst 4966-76 was 1.5 nm. However, some larger particles, i.e., 4 nm were also present.

Catalyst 4966-96-2 with ~1% Ru (by wt.) and ~0.7% K (by wt.) had over 90% of the visible ruthenium particles in the 2-4 nm size range according to STEM examination, while the remainder of the particles were 4-15 nm (Figures 5-67 and 5-68). Catalyst 4966-96-2 also showed a bimodal size distribution in the EXAFS examination: while the average ruthenium particle size was 1 nm, particles as large as 3 nm were also present. The  $H_2:Ru$  ratio was 0.27.

Since the number of observed ruthenium particles were much less than expected for these three catalysts, a significant fraction of the ruthenium particles probably were smaller than 2 nm, and, therefore, invisible with STEM.

#### 5.1.3.2.3 Ruthenium Catalyst on Titania

Catalyst 4966-106 with ~1% Ru (by wt.) was prepared on titania (anatase) and had ruthenium particles in the 3-10 nm size range according to STEM (Figures 5-69 and 5-70). The ruthenium particle size distribution was not determined in more detail because of the difficulty of distinguishing small titania crystallites from ruthenium. According to EXAFS, the ruthenium particle size was 2-3 nm.

#### 5.1.3.2.4 Ruthenium Catalyst on Alumina-Titania

Catalyst 4966-124 with ~1 Ru (by wt.) was prepared on an alumina-titania support (1:1 by wt.) and had, according to STEM examination, flat plate-like ruthenium particles in the 25-50 nm size range (Figures 5-71 and 5-72).

Figure 5-66  
STEM Micrograph of Catalyst 4966-76

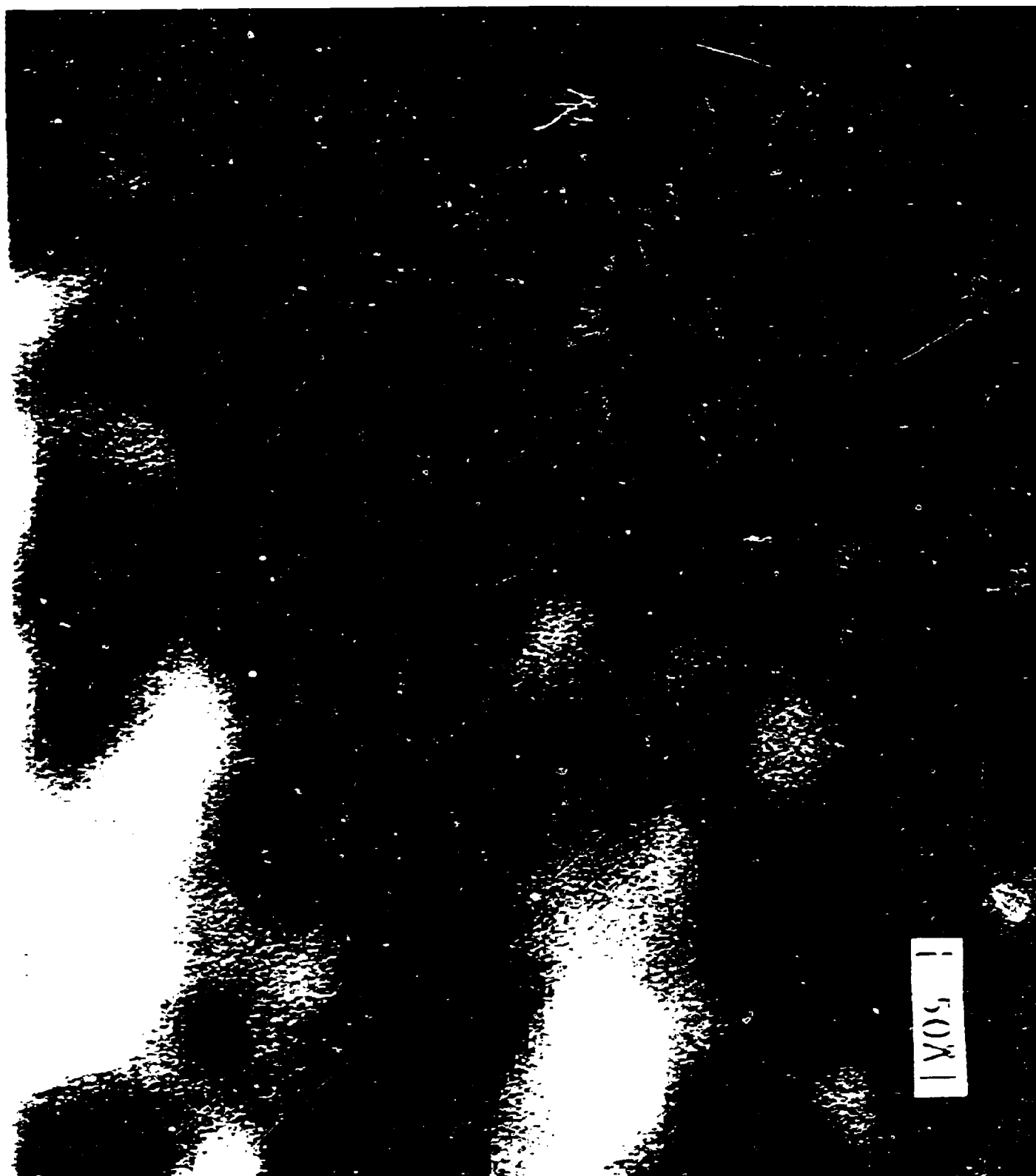






Figure 5-67. STEM Micrograph of Catalyst 4966-96-2

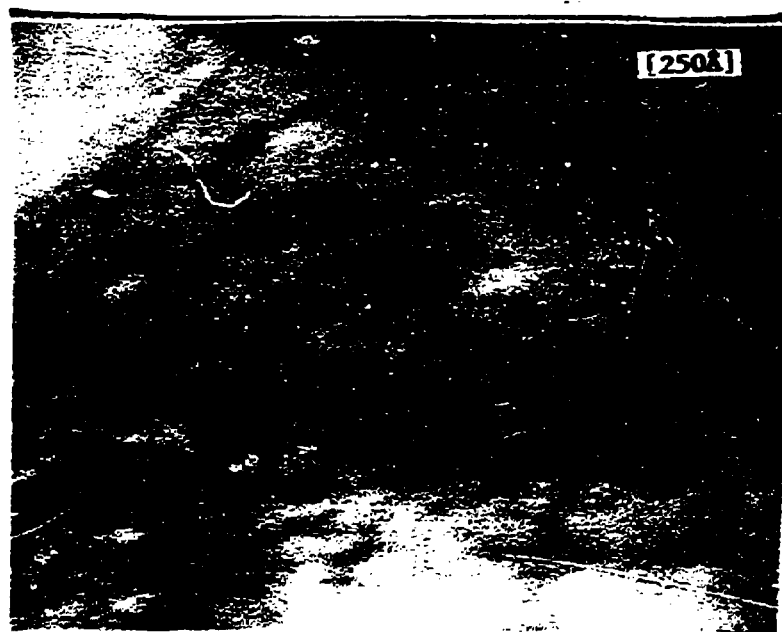


Figure 5-68. STEM Micrograph of Catalyst 4966-96-2



Figure 5-69. STEM Micrograph of Catalyst 4966-106

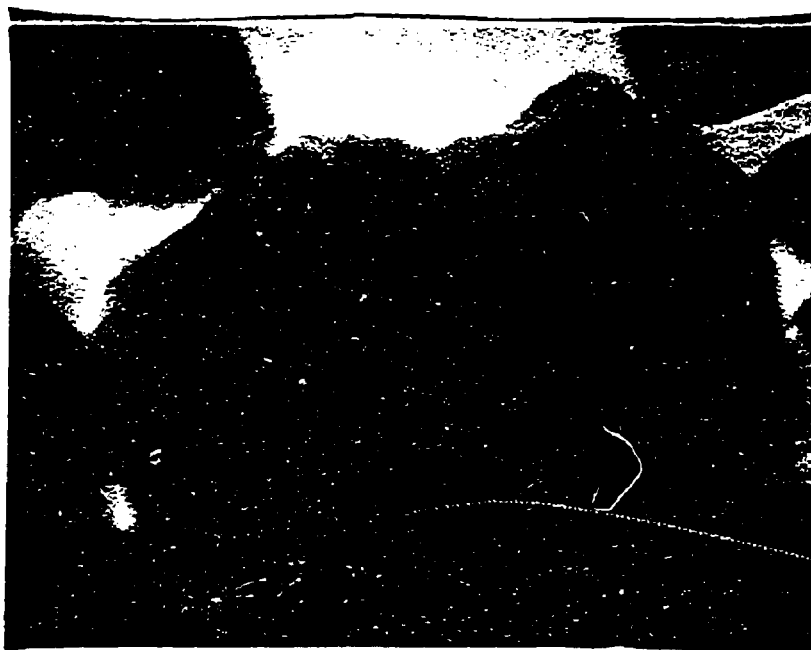


Figure 5-70. STEM Micrograph of Catalyst 4966-106

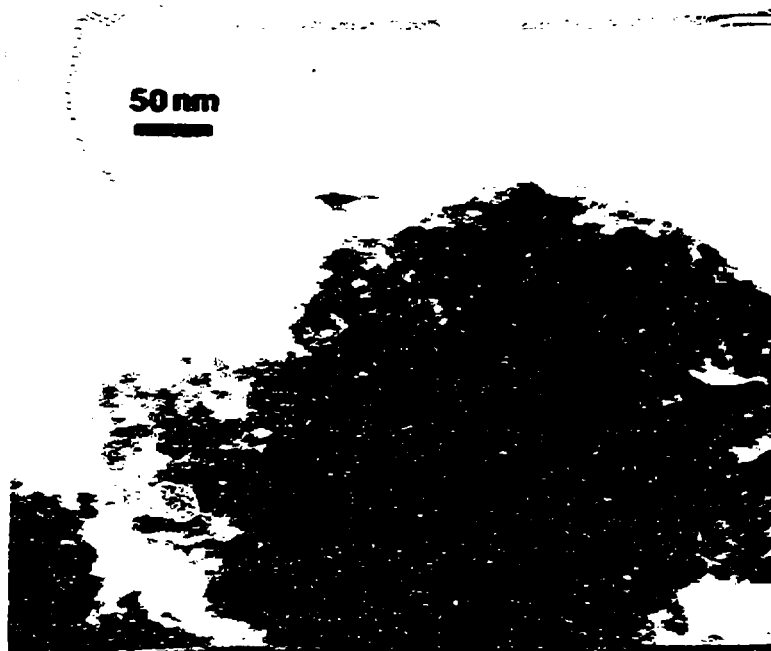


Figure 5-71. STEM Micrograph of Catalyst 4966-124

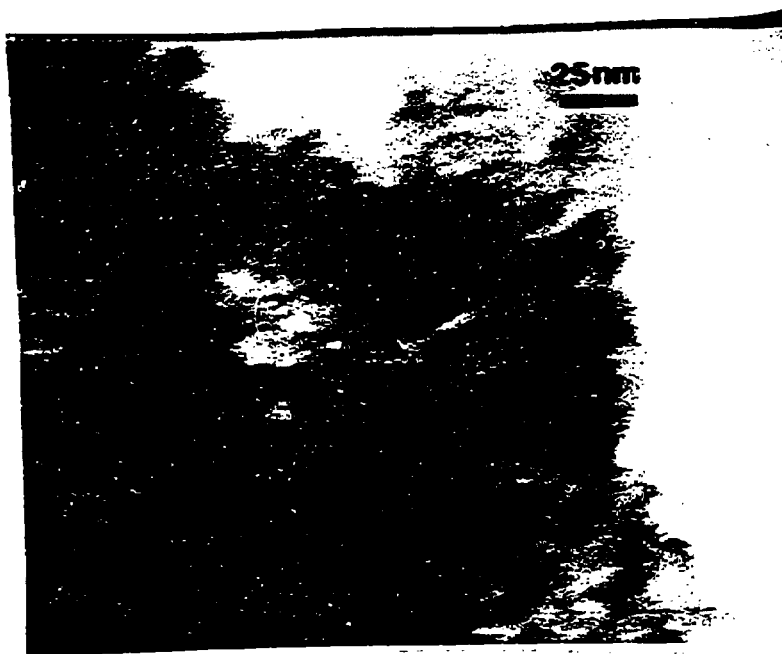


Figure 5-72. STEM Micrograph of Catalyst 4966-124

#### 5.1.3.3 XRD Examination of Ruthenium Catalysts Prepared by Reverse Micelles

The samples were transferred to an "o" ring sealed diffraction cell with a Kapton window in a glove box to maintain an inert atmosphere. Measurements were made on the Rigaku diffractometer with a Mo x-ray source. Test scans of Ru metal powder (4956-34) spread onto the back of a piece of Kapton tape, and scans of an  $\gamma$ -alumina powder and a physical mixture of 10% Ru powder (>325 mesh) with a  $\gamma$ -alumina powder (4956-46), were made in order to identify the Ru peaks best suited for the lineshape analysis. These scans are shown in Figures 5-73 through 5-75.

As can be seen in these figures, there is a strong overlap of the sharp features of the relatively large Ru crystallites in the powder and the gamma-alumina material. It was, therefore, not clear whether it would be possible to separate the broad bands expected for the small Ru crystallites from the background. A long time scan of Catalyst 4956-21 is shown in Figure 5-76. No evidence for any Ru features can be found. Even if relatively large crystallites are present, it is doubtful that an easy separation of the background from the Ru peaks could be effected. In this case, where small crystallites with broad peaks are expected, the use of x-ray lineshape analysis can be completely ruled out.

Since the x-ray lineshape method is a very useful method for information about the distribution of sizes over a broad range without microscopic examination of many individual crystallites, a second catalyst on a gamma-alumina support was tried. Only small quantities of this catalyst (4956-19) were available so that the normal cell loading procedure could not be used. A small portion of the catalyst was spread evenly on the back of a piece of Kapton tape on a normal sample slide. This required a measurement in air. Also, since only a very small amount of material was present, a long scan time was required

Figure 5-73. XRD Measurements on Ruthenium Metal Powder (4956-34)

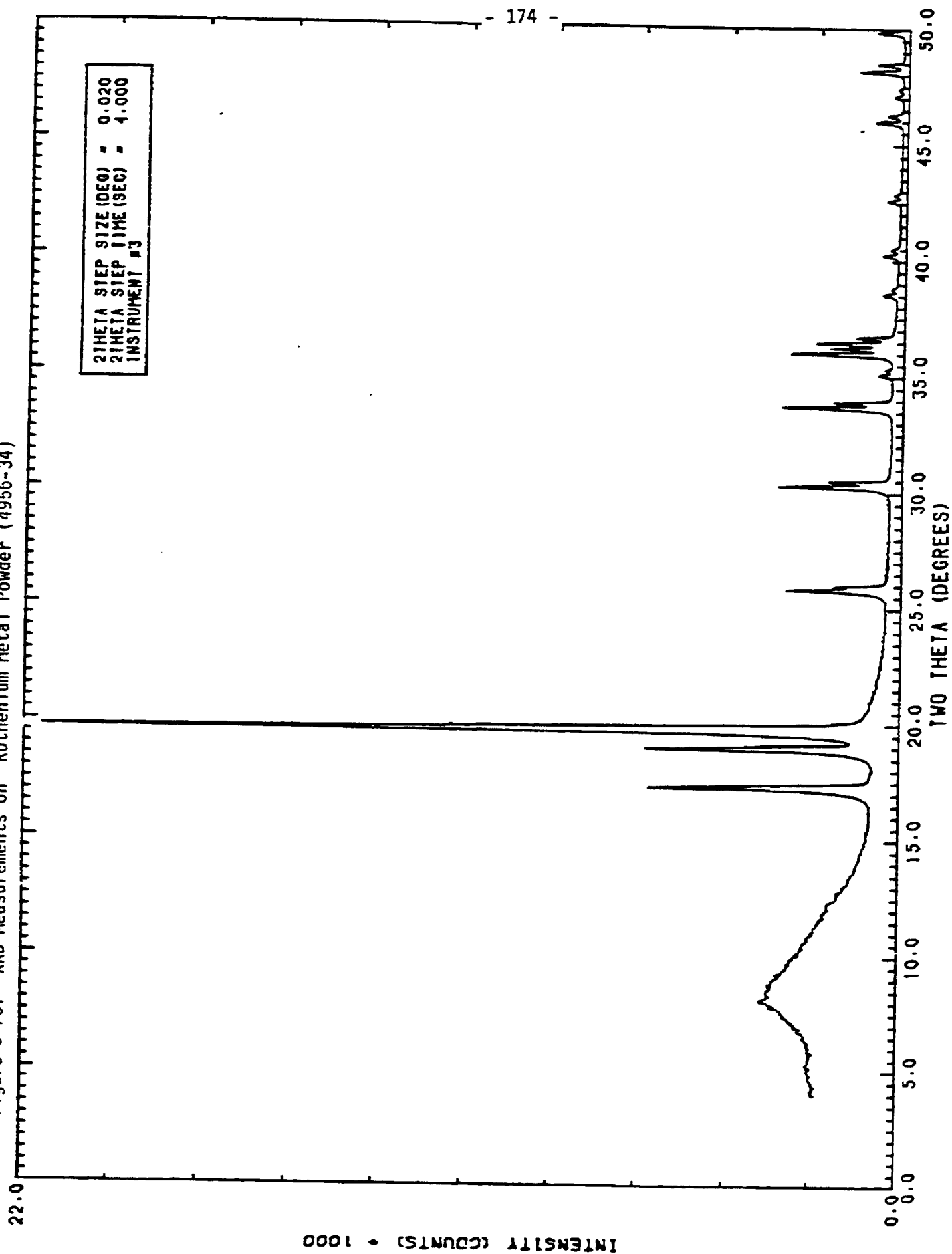


Figure 5-74. XRD Measurements on  $\gamma$ -Alumina Support

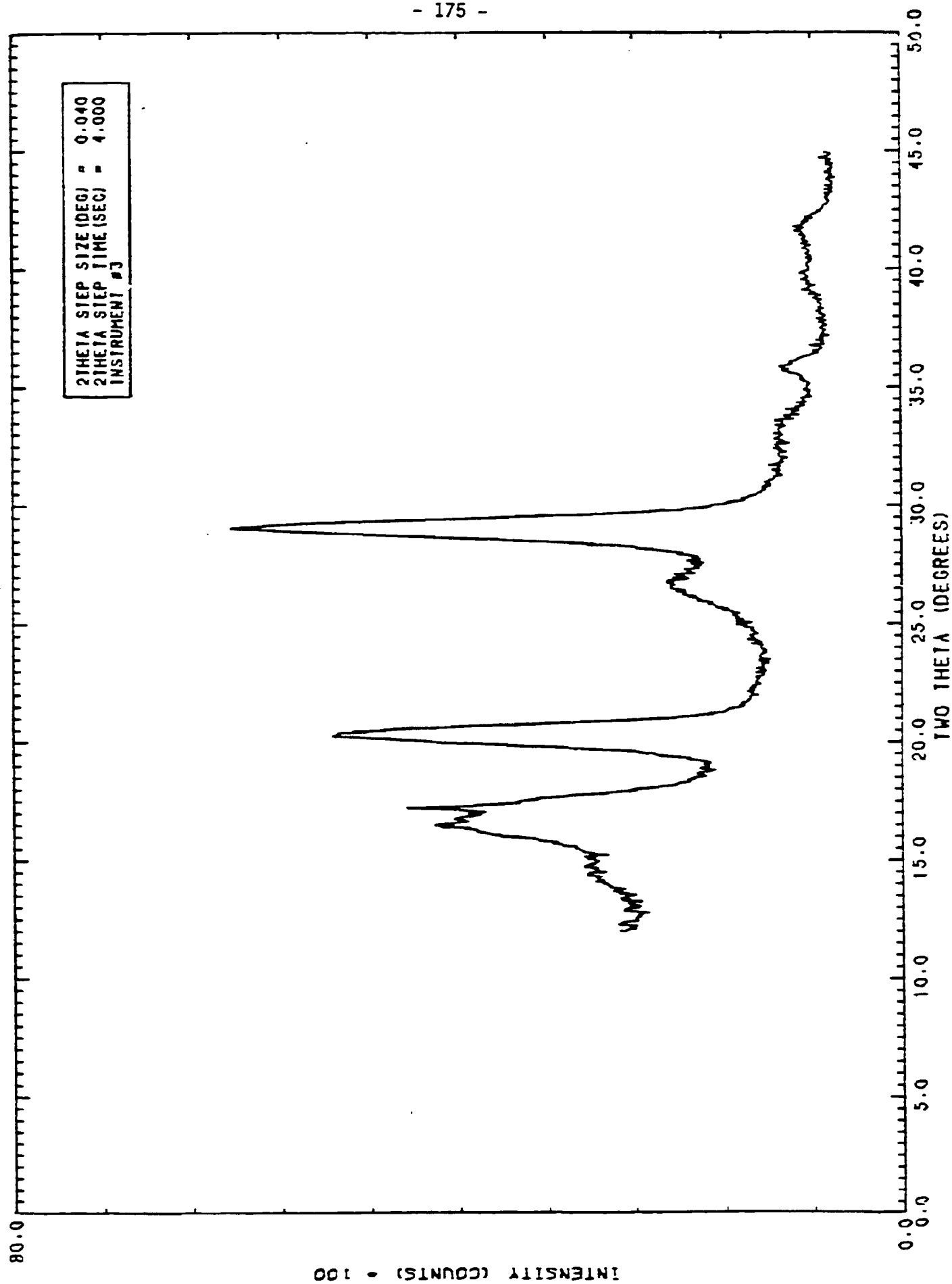


Figure 5-75. XRD Measurements on a Physical Mixture of Ruthenium Metal Powder with  $\gamma$ -Al<sub>2</sub>O<sub>3</sub>  
(1:10, by wt.)

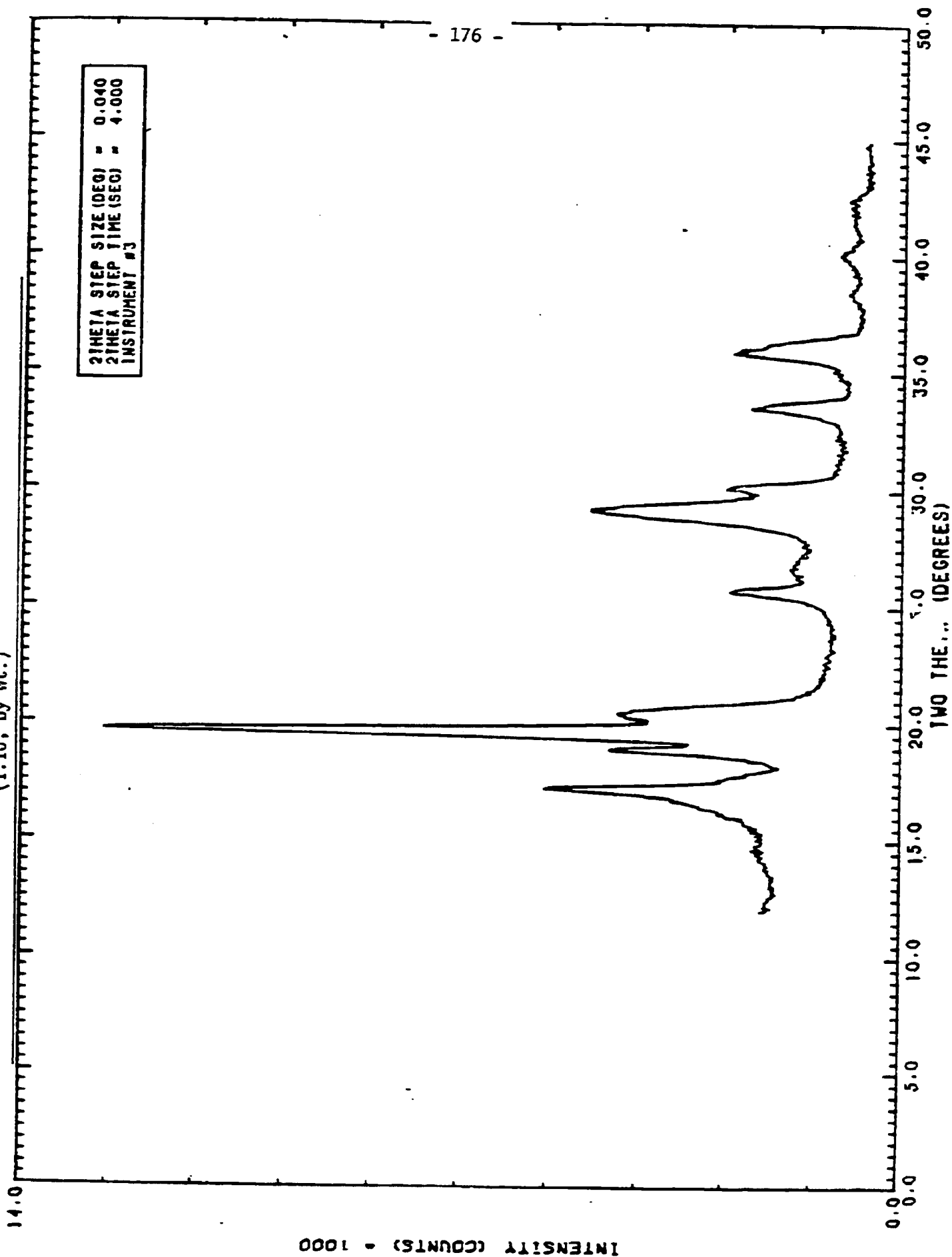
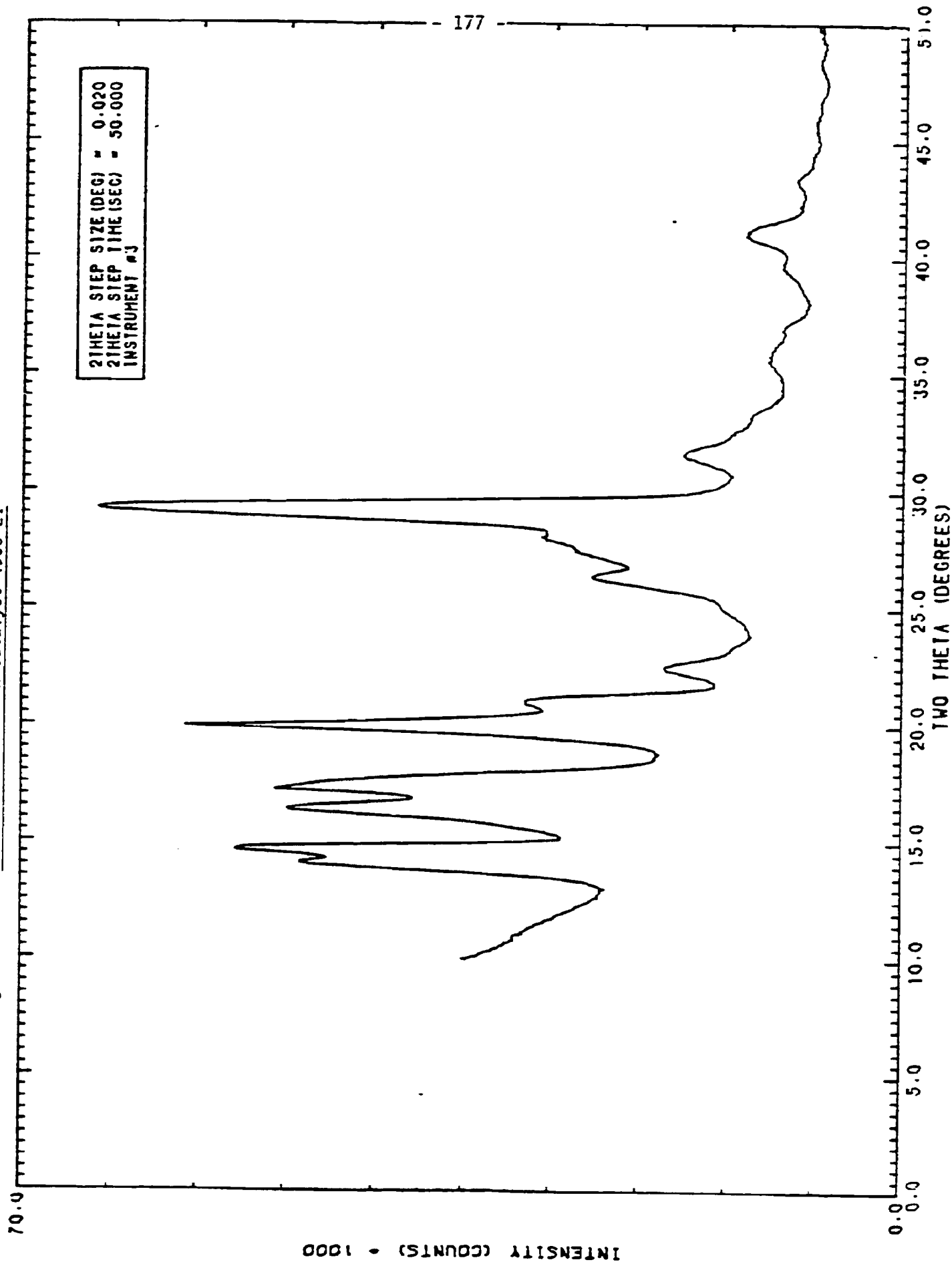


Figure 5-76. XRD Measurements on Catalyst 4956-21





in order to obtain even qualitative information. The results are shown in Figure 5-77. The steep sloping background in the catalyst sample is due to scattering from the Kapton tape itself. There is good correspondence for each catalyst feature with features in the  $\gamma$ -alumina support only. (Two additional features can be seen in a number of the scans at  $17.2^\circ$  and  $20^\circ$ ; these are due to the beam catching part of the sample holder.) Thus, Ru is again not detectable. Even though there is only a small amount of sample, the signal-to-noise ratio of the catalyst is clearly high enough to allow identification of the Ru features if they were visible.

Since the scan for Catalyst 4956-19 was done in air, and air sensitivity may be a problem with reduced Ru catalysts, the question of possible oxidation of the metal to  $\text{RuO}_2$  must be considered. A scan of  $\text{RuO}_2$  spread on Kapton tape is shown in Figure 5-78. The pattern has two strong peaks at low angle which should not be obscured in any of the other scans. Since no features are found in this range in the catalyst, it is concluded that crystalline  $\text{RuO}_2$  is not present in a significant amount.

#### 5.1.4 Application of Conventional Aqueous Impregnation to the Preparation of Highly Dispersed Ruthenium Catalysts

Three catalysts were prepared by conventional aqueous impregnation techniques in order to form highly dispersed ruthenium (see Table 5-2). Catalyst 4956-86 with 1.06% Ru (by wt.) was prepared by impregnation with a  $\text{RuCl}_3 + \text{HCl}$  solution onto alumina, followed by drying at  $110^\circ\text{C}$  and reduction with  $\text{H}_2$  at  $500^\circ\text{C}$ . Catalyst 4966-72 with 1.05% Ru (by wt.) was prepared by impregnation with another aqueous ruthenium solution onto alumina, followed by drying at  $110^\circ\text{C}$ , calcination at  $300^\circ\text{C}$  and reduction with  $\text{H}_2$  at  $380^\circ\text{C}$ . Catalyst 5345-61 with 0.93% Ru (by wt.) was prepared onto titania (anatase) by a procedure similar to that used for Catalyst 4966-72.

Figure 5-77. XRD Measurements on Catalyst 4956-19

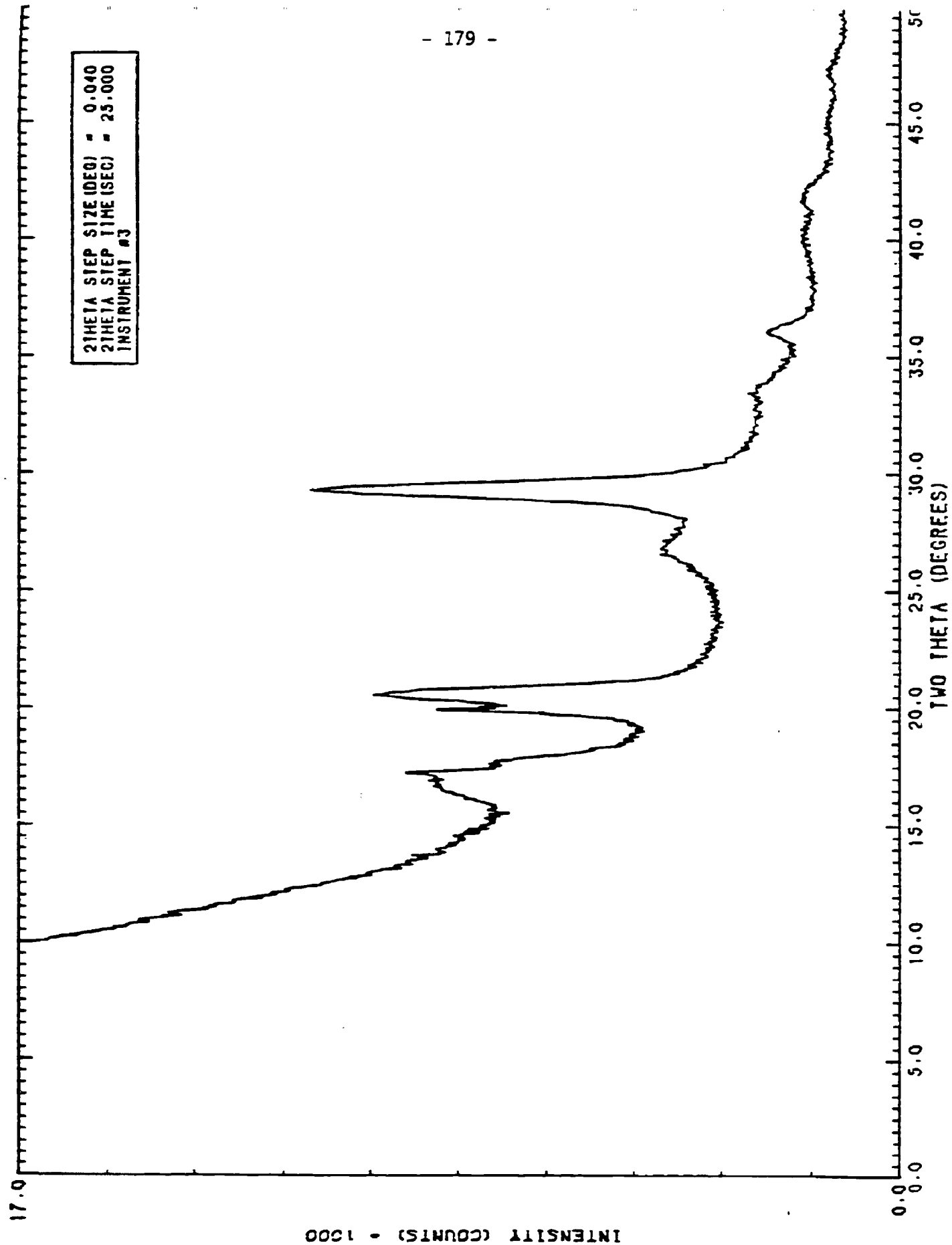


Figure 5-78. XRD Measurements on RuO<sub>2</sub> Powder

